Electron-spin relaxation and molecular dynamics in liquids. I. Solvent dependence[a)]

Stephen A. Zager and Jack H. Freed

Baker Laboratory of Chemistry, Cornell University, Ithaca, New York 14853
(Received 26 March 1982; accepted 4 June 1982)

Temperature-dependent ESR relaxation studies of PD-Tempone in a variety of solvents ranging from weakly interacting hydrocarbons to strongly interacting D_2O are described. The empirical molar transition energy scale E_T, which is a good measure of specific solvent polarity, is found to lead to a useful interpolation method for estimating the solvent dependence of the magnetic tensors required for accurate spin-relaxation studies. The temperature-dependent results are generally well-represented by a modified Stokes–Einstein type of η/T dependence for τ_R, the rotational correlation time. The ϵ parameter introduced by Freed and coworkers as an empirical correction to the nonsecular Debye spectral densities is found to correlate with E_T, such that it is largest for the weakly interacting hydrocarbon solvents and approaches the Debye limit of $\epsilon = 1$ for D_2O solvent. This is discussed in terms of approximate fluctuating torque and slowly relaxing local structure models, and the former appears more consistent with experiment. It is also pointed out that $\epsilon > 1$ would result from the phenomenological feature of viscoelasticity.

I. INTRODUCTION

Hwang, Mason, Hwang, and Freed[1] (HMHF) have shown the value of ESR relaxation studies with a relatively small and deuterated spin probe (cf. Fig. 1) in the study of molecular reorientational dynamics in ordinary liquids. It is small enough that one expects and detects significant deviations from Brownian motional models. These appear as significant deviations from Debye spectral densities of the high-frequency (or nonsecular) relaxation contributions in the motional narrowing region and as line shape characteristics in the slow motional region which are particularly sensitive to reorientational model.[1,2] These are features not usually observed with larger probe molecules such as VOAA.[3,4] Although there are other important physical techniques for studying rotational dynamics in liquids,[5,6] these features of ESR relaxation studies appear to be rather special.

In this work we report on further studies we have performed with PD-Tempone in a variety of isotropic solvents in recent years which amplify important aspects of the rotational dynamics of this probe. Some of this work was undertaken for comparison with studies of molecular dynamics in liquid crystalline solvents,[7] and preliminary reference may be found in those reports.[7(c)] In particular, we examine in this work: (1) the solvent dependence of ϵ, which characterizes the non-Debye spectral density:

$$j(\omega) = \tau_R/(1 + \epsilon\omega^2\tau_R^2) \ , \tag{1}$$

found useful in previous work[1,2,7]; (2) the validity of a Stokes–Einstein type of law, by which we mean a

$$\tau_R \propto \eta/T \ , \tag{2}$$

for this probe in a variety of solvents. Many studies in recent years have focused on the question of the applicability of modified Stokes–Einstein behavior for small molecules in liquids, and this topic has recently been extensively reviewed.[4,5] We also consider related matters of spin-rotational relaxation and some other anomalous features of the spin relaxation.

Some interesting correlations emerge from this study of solvent dependence. In particular, we wish to emphasize the solvent polarity as an important parameter. The "effective" polarity of a solvent depends on a variety of intermolecular forces as well as specific (hydrogen) bonding between the solvent and the solute. Lin and Freed[7(c)] have employed a particular empirical method based upon the extensively studied molar transition energy scale E_T.[8] They found the E_T scale very useful for representing solvent variations of hyperfine splittings a_N (and a_D), and this has now led to a comprehensive measure of solvent polarity specific to the PD-Tempone probe. The various features of rotational dynamics of this probe could then be compared with this parameter as well as more familiar ones (e.g., solvent size).

Another virtue we have found of the E_T scale for ESR studies is that the hyperfine and g-tensors, which are sensitive to solvent, scale rather well with this parameter. Thus, good estimates of these tensors can often be obtained without the necessity of performing careful simulations of rigid limit spectra in the particular solvent. The latter is often beset with poor resolution

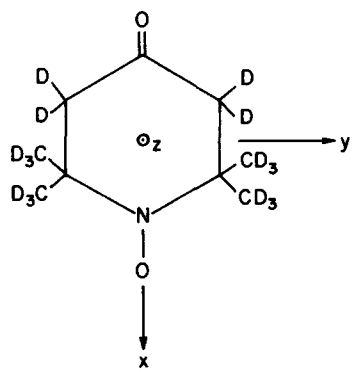

FIG. 1. Perdeuterated 2,2,6,6-tetramethyl-4-piperidone *N*-oxide (PD-Tempone) showing molecular-fixed axis system.

[a)]Supported by NSF Grant No. CHE 8024124.

 0021-9606/82/193344-16$02.10

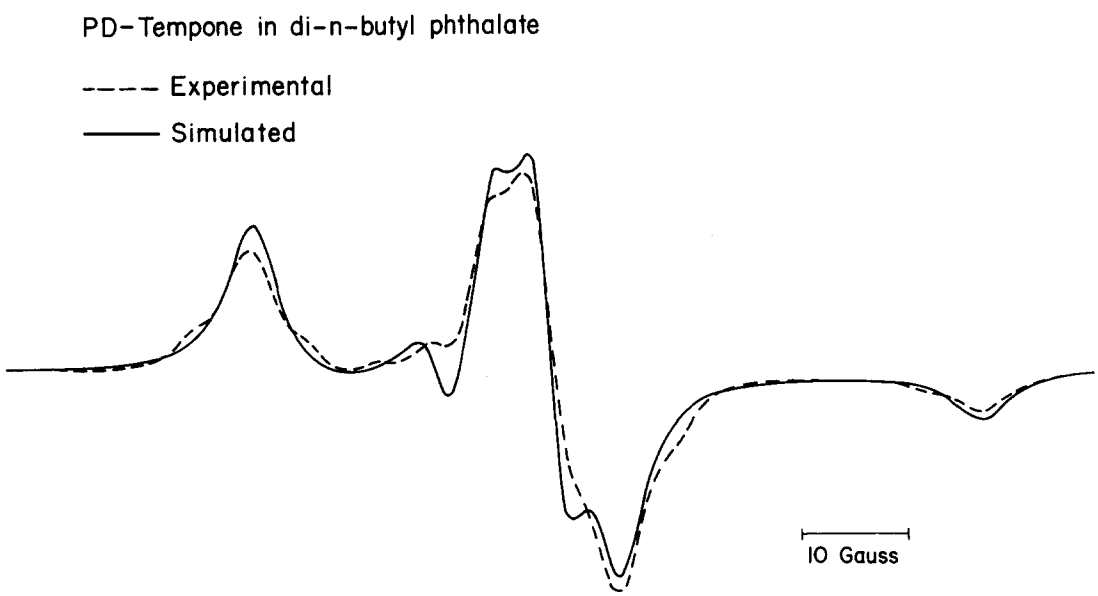

FIG. 2. Rigid limit spectrum of PD-Tempone in di-*n*-butyl phthalate. Simulation based on magnetic parameters given in Table I.

from inhomogeneous broadening, and in many solvents the probe does not remain magnetically dilute upon freezing, because it can precipitate out. We analyze and use this scaling procedure in the present work.

The emphasis in the present work is on solvent effects on molecular dynamics from temperature-dependent studies at atmospheric pressure. In a companion work[9] we consider the molecular dynamics of the PD-Tempone probe in a single solvent, but as a function of both temperature and density, and the matters of Stokes–Einstein behavior and non-Debye spectral densities are critically examined from that viewpoint.

II. EXPERIMENTAL CONSIDERATIONS

All ESR measurements were made at *X* band with a Varian E-12 Spectrometer system using 10 kHz field modulation and a Varian E-4531 multipurpose cavity. The Varian E-257 variable temperature accessory produced temperatures typically regulated to within ± 0.5 °C. To determine the sample temperature, a copper-Constantan thermocouple, fixed in the active region of a standard sample tube filled with liquid solvent, was placed in the microwave cavity before and after each set of measurements. As a function of temperature, complete ESR line shapes were collected on line as described elsewhere.[10] The effects of excessive magnetic field modulation and microwave power saturation were guarded against by frequent checks and adjustments. The nitroxide-free radical: perdeuterated 2, 2, 6, 6-tetramethyl-4-piperiodone N-oxide (PD-Tempone) shown in Fig. 2 was synthesized by Dr. Bogumil Hetnarski following procedures used previously.[1] Solutions of PD-Tempone were prepared volumetrically in a desiccated nitrogen glove bag and transferred to conventional Pyrex sample holders[11] for subsequent vacuum line freeze-pump-thaw degassing. After being sealed under vacuum, the sample holders were refrigerated, and solution-filled sidearms were withdrawn as needed. For each solvent, several spin-probe concentrations were tested to avoid exchange broadening. All samples demonstrated excellent stability; the same sample tubes were used more than a year later in supplemental experiments.

Di-*n*-butyl phthalate (DNBPT) (Eastman Organic Chemicals), D_2O (Aldrich Chemical Company, 99.8 at. % D), *n*-decane (Aldrich Chemical Company), and *n*-dodecane (Eastman Organic Chemicals) were used with PD-Tempone concentrations ranging from 1×10^{-5} to 1×10^{-3} M. Sample tubes were ordinarily made from standard 3 mm Pyrex tubing; we used 1 mm capillary Pyrex tubing for D_2O solutions along with careful sample positioning to minimize microwave dielectric loss and to achieve symmetric ESR line shapes.

Viscosities were interpolated and extrapolated using available data and standard empirical relations.[12] For temperatures below 35 °C, the viscosity of DNBPT was calculated from[12]

$$\ln\eta = -8.396 + \frac{966.7}{T - 151.3} \tag{3a}$$

(which is in the form of a Doolittle equation[12]), where η is the viscosity in poise and T is in K. From available data[12] we found that for temperatures above 35°,

$$\ln\eta = -7.790 + \frac{880.6}{T - 151.3} \ . \tag{3b}$$

The viscosity of D_2O[13] was calculated from[14]

$$\log(\eta/1.2471) = [1.3580(20 - t) - 0.000\,67(t - 20)^2]/(t + 96.71) \ , \tag{4}$$

where η is the viscosity in cP and t is the temperature in °C. This expression was given for the 5–70 °C range, but we have compared the predictions to high temperature measurements[15] and recent low temperature results[16] and found less than 2% deviation across

our experimental temperature range. For the hydrocarbon solvents we used available viscosity data.[17]

The Varian E-12 ESR spectrometer was interfaced to a PRIME 400 timeshared computer, and interactive software was developed to collect, interpret, and store individual spectra.[10] From measurements of a complete experimental line shape (enhanced by signal averaging when needed), the derivative peak-to-peak width and height as well as the asymmetry of the line was determined using an efficient fifth-order polynomial curve-fitting scheme.[18] The observed line shapes include some inhomogeneous broadening due to unresolved super-hyperfine splitting from twelve equivalent methyl deuterons (with smaller splittings from the ring deuterons). Initially, simulations of the complete line shape were performed to obtain accurate values of a_D and intrinsic homogeneous width.[10] Since a_D was generally found to be constant for each solvent and independent of temperature, we then used tabulations of the intrinsic width, the observed width, and the observed peak-to-peak height (where the linewidths are given in units of a_D) to obtain the intrinsic widths. These intrinsic linewidths are expressed as a quadratic in $\tilde{M}_I$, the z component of the N^{14} nuclear spin quantum number:

$$\delta(\tilde{M}_I) = A + B\tilde{M}_I + C\tilde{M}_I^2 \ . \tag{5}$$

In practice, one linewidth and two relative peak heights were used to determine A, B, and C, since the experimental error in the peak heights is typically 0.1%, while the linewidths are uncertain by about 1%. Thus the relative values of A, B, and C are determined more accurately than their absolute values. (The other two measured linewidths were used to check on the accuracy of the experimental results and the analysis). Further details are given by Zager.[10]

III. RESULTS

A. Rigid limit magnetic parameters

1. PD-Tempone in di-n-butyl phthalate

The rigid limit spectrum of PD-Tempone in DNBPT at −150 °C is shown in Fig. 2. Our best computer simulation[19] is also shown, and the resulting magnetic parameters are given in Table I. These values are comparable to those found for PD-Tempone in several perdeuterated organic solvents, being especially close to those determined in acetone-$d6$.[1] This similarity is also seen in the angular dependent residual Lorentzian linewidth coefficients $\alpha = 2.22$ G and $\beta = 1.5$ G. Although unresolved intramolecular deuterium hyperfine interactions may be important in these widths, intermolecular dipolar interactions with solvent protons should also be contributing. Consistent with this, the deuteron hyperfine splitting constant a_D, obtained from line shape simulations in the motional narrowing region, appears slightly *larger* in this protonated solvent.

2. PD-Tempone in D_2O: The scaling method for magnetic tensors

Attempts at obtaining the rigid limit spectrum of PD-Tempone in D_2O were unsucessful. Both rapid and slow cooling to the frozen state at several low temperatures gave a broad singlet ESR spectrum. This observation is consistent with nitroxide agglomeration; with strong spin exchange and/or dipole–dipole interactions collapsing the spectrum to a single line. A similar nitroxide radical in frozen H_2O has shown this effect.[20] A proper analysis of linewidth data in the motionally narrowed region depends upon accurate magnetic parameters. Lacking the unambiguous assignment provided by a rigid limit spectral simulation, we developed an alternate method to determine the magnetic parameters for PD-Tempone in D_2O. We were, shortly thereafter, able to check the predictions of this method against other results.[21]

Our method is based on the observed linear relation between the isotropic hyperfine splitting constants, a_N and a_D, for PD-Tempone and the molar transition energy E_T of the solvent,[7(c)] which is a measure of the solvent polarity.[8] PD-Tempone is chemically inert in the solvents under consideration, but solvent complex formation affects the unpaired electron density at the N–O fragment and therefore, the measured hyperfine splitting constants. Indeed for PD-Tempone we found that the *individual components* of both the **g** and **A** tensors correlate with the molar transition energy.

In Table I we present the data that allow one to establish these correlations. The elements of the magnetic tensors were taken from the results of rigid limit measurements and simulations of PD-Tempone in polycrystalline matrices. Values of a_N, a_D, and Δg_s were obtained in the motional narrowing region and in the isotropic phase for anisotropic liquids. The E_T values were then obtained from the linear relation between E_T and a_N already found for solvents for which both E_T and a_N were known.[7(c)] With this extensive listing of E_T values, it was possible to verify linear relations between E_T and the magnetic tensor components given in Table II. (In examining these relations it is important to consider the estimated experimental uncertainties in the magnetic parameters. Some parameters showed more scatter than others, but linear equations were found to represent their E_T dependence adequately.)

We note, in passing, that the fully protonated spin probe Tempone has been studied in a variety of isotropic liquids, including aqueous solutions of mixtures of hydrophobic solutes,[22] common organic solvents,[23] and water–phospholipid mixtures and model systems.[21] These data could be used to perform an accurate E_T analysis analogous to that which we performed for PD-Tempone, and one would expect similar results.

3. PD-Tempone in n-decane and in n-dodecane

We were unable to obtain rigid limit spectra for PD-Tempone both in n-decane and n-dodecane. Instead, single line ESR spectra were observed. In our linewidth analyses we simply utilized the magnetic parameters for PD-Tempone in toluene-$d8$ given the closeness of the E_T values of these solvents (cf. Table I). (The predicted parameters for PD-Tempone in n-decane and n-dodecane are themselves virtually identical and would differ from those given for PD-Tempone in toluene-$d8$

TABLE I. Magnetic parameters and molar transition energies for PD-Tempone in isotropic solvents.

Solvent	E_T (kcal/mol)[a]	a_N (G)	A_x (G)	A_y (G)	A_z (G)	a_D (mG)	Δq_s[b]	Δq_x[b]	Δq_y[b]	Δq_z[b]
n-dodecane	(30.6)	14.39 ± 0.02				28.7 ± 0.2				
n-hexane[c]	30.9	14.39								
n-decane	(30.9)	14.40 ± 0.02				27.1 ± 0.2				
paraffin oil[d]	(32.5)	14.46			32.5		3.76			
CCl_4[e]	32.5	14.48								
toluene-*d*8[f]	(35.8)	14.572 ± 0.015	4.1 ± 0.5	6.1 ± 0.5	33.45 ± 0.2	20.5 ± 0.2	3.70 ± 0.05	7.28 ± 0.2	3.98 ± 0.2	−0.12 ± 0.1
8CB[g]	(36.6)	14.60 ± 0.02			33.3 ± 0.3		3.70 ± 0.2			
di-*n*-butyl phthalate	(38.5)	14.67 ± 0.02	4.9 ± 0.5	5.5 ± 0.5	33.6 ± 0.6	23.3 ± 0.2	3.69 ± 0.05	7.18 ± 0.3	3.88 ± 0.3	−0.12 ± 0.3
40,6[a]	(39.4)	14.70 ± 0.02			33.5 ± 0.3	22.9 ± 0.6	3.70 ± 0.2			
BOCP[h]	(40.6)	14.74			33.9					
phase IV[h]	(40.9)	14.75			33.5		3.70			
phase 7-*A*[d]	(41.2)	14.76			33.4		3.69			
phase V[h]	(41.7)	14.78 ± 0.02	5.61 ± 0.2	5.01 ± 0.2	33.7 ± 0.3	21.5 ± 0.5	3.69 ± 0.05	7.38 ± 0.2	3.88 ± 0.2	−0.17 ± 0.1
BEPC[h]	(42.0)	14.79			33.8		3.68			
acetone-*d*6[f]	42.2	14.742 ± 0.015	4.8 ± 0.5	5.4 ± 0.5	34.0 ± 0.3	22.4 ± 0.2	3.66 ± 0.05	7.18 ± 0.3	3.88 ± 0.3	−0.12 ± 0.2
oleic acid[d]	(42.3)	14.80			34.2		3.68			
decanoic acid[d]	(46.3)	14.94			34.9					
DPL[d]	(49.2)	15.04			34.2					
egg lecithin[d]	(49.5)	15.05			34.1		3.67			
ethanol-*d*6[f]	51.9	15.173 ± 0.015	4.75 ± 0.6	5.65 ± 0.6	35.1 ± 0.4	20.2 ± 0.2	3.57 ± 0.05	6.88 ± 0.4	3.78 ± 0.4	−0.12 ± 0.3
methanol[c]	55.5	15.26								
85%-glycerol-*d*3-D_2O[f]	(69.4)	15.740 ± 0.015	5.5 ± 0.5	5.7 ± 0.5	35.8 ± 0.3	16.0 ± 0.2	3.38 ± 0.05	6.08 ± 0.2	3.68 ± 0.2	−0.12 ± 0.1
H_2O[d]	(81.8)	16.17			36.6		3.28			
D_2O	(81.8)	16.173 ± 0.05	(5.67)	(5.64)	(36.9)	12.4 ± 0.3	3.27 ± 0.1	(5.68)	(3.58)	(−0.12)
20%-glycerol-H_2O[d]	(82.0)	16.18			36.45		3.30			

[a]From Ref. 8. Values in parentheses were calculated in this work from a_N.
[b]$\Delta g_i \equiv 1000\ (g_i - 2.002\,32)$.
[c]W. J. Lin (unpublished results).
[d]From Ref. 21.
[e]J. S. Hwang (unpublished results).
[f]From Ref. 1.
[g]From Ref. 7(c).
[h]From Ref. 7(a).
[i]Interpolated magnetic parameters in parentheses.

TABLE II. Summary of results on rotational relaxation of PD-Tempone vs solvent properties.

Solvent	E_T	r_s, Å	$\kappa^{1/3}$	$\tau_R^0 \times 10^{12}$ s	ϵ	ϵ'	N	V_s cm^3 [g]
n-dodecane[a]	30.6	1.28±0.02	0.400	7.3±3.5	10		$2y$	227.4
n-decane[a]	30.9	1.51±0.02	0.472	1.6±0.3	6.25		$1.5y$	194.9
CCl_4[b]	32.5	1.62	0.506	1.3	6		1	96.9
Toluene-$d8$[c]	35.8	2.0	0.625	−0.2±0.3	5.4	(1–4)	1	106.3
8CB[d]	36.6	···	···	···	[~3–4]		1	291[h]
DNBPT[a]	38.5	1.47±0.01	0.460	0.3±0.3	4	12	$2.1x$	265.9
40, 8[d]	39.4	···	···	···	[~4.5–7]		[~$1.6y-1$]	~365[h]
MBBA[e]	42	~1.13	0.353	···	4.6		1	260[h]
Acetone-d_6[f]	42.2	1.90	0.907	−6.2	2.5		$1.7y$	73.5
Ethanol-d_6[f]	51.9	2.30	0.721	−13	3.4	>1	$3x$	58.4
85% glycerol-D_2O[f]	69.4	1.74	0.543	−21	···	~4	~1	89.3
D_2O[a]	81.8	2.27±0.01	0.709	$(-0.2\pm2.8)\times10^{-2}$	1.1		$1.6x$	18.1

[a]This work.
[b]J. S. Hwang (unpublished).
[c]From Ref. 9.
[d]From Ref. 7(c). The limits on 40, 8 are given by the pairs $\epsilon=4.5$ and $N=1$ or $\epsilon=7$ and $N=1.6y$.
[e]From Ref. 7(a).
[f]From Ref. 1.
[g]Molar volume for protanated solvent at 20°C. Most of entries are from *Handbook of Chemistry and Physics*, 54th Ed. (CRC, Cleveland, 1973–1974). See h for others.
[h]The benzilidene liquid crystals were found to have a specific volume very close to 1 cm^3/g at the nematic-smectic phase transition [B. Bahadur, J. Chem. Phys. **73**, 255 (1976)].

by less than twice the reported experimental error. Over the τ_R range used this would lead to an experimentally insignificant 1%–2% increase in the theoretical values of B and of C.)

B. Linewidths and relaxation times

1. Definitions and procedures

Analysis of the ESR linewidth results in the motional narrowing region proceeded in the standard manner.[1,2] First, the experimental linewidths were reduced to the intrinsic linewidth coefficients A, B, and C, (cf. previous section). Second, the resulting B and C values were used to determine the relaxation parameters discussed below.

The mean rotational correlation time $\tau_{\bar{R}}$, was determined as follows: First the experimental values of C were plotted against those of B; then, using the theoretical expressions for B and C[1,2] the parameters N, ϵ, and ϵ' were adjusted to find the combination that best described the data. These parameters can most easily be optimized one at a time over different ranges of $\tau_{\bar{R}}$ and their temperature independence checked. Of course only if linewidth measurements are made over a sufficiently wide range of $\tau_{\bar{R}}$ values can N, ϵ, and ϵ' be obtained in such a manner. Here N characterizes axially symmetric rotational diffusion: $N=R_\parallel/R_\perp$, where $R_\parallel$ is the principal component of the rotational diffusion tensor about the symmetry axis z' and $R_\perp$ is the corresponding principal component about the x' and y' axes. Finally, we have $\tau_{\bar{R}} \equiv (6R_\parallel R_\perp)^{-1}$,[24(a)] so in the limit of isotropic rotation, $N=1$ and we let $\tau_{\bar{R}}=\tau_R$. The local symmetry of the N–O fragment in PD-Tempone implies that the molecule-fixed x, y, z axis system is (nearly) equivalent to the x', y', z' axis system to within a permutation of the axis labels. Figure 1 shows the molecule fixed coordinate system for PD-Tempone. Both $x'=x$ and $z'=y$ assignments have been found for PD-Tempone in isotropic liquids with corresponding N values ranging from 1–3 (cf. Table II).

We illustrate the analysis with the motional narrowing linewidth data for PD-Tempone in DNBPT. The determination of $\tau_{\bar{R}}$ follows from Fig. 3. The theoretical curves of B vs C are sensitive to N over the entire experimental range, but in the region $100<B(\text{mG})<600$ they are independent of the values of ϵ and ϵ' and form a family of parallel lines for different values of N; (we distinguish the ϵ correction to the nonsecular and the pseudosecular spectral densities by ϵ and ϵ', respectively). Thus N can be assigned from this data subset; x-axis orientation of the rotational diffusion tensor with $N=2.1$ accurately represents the data. The remaining parameters are readily established, since for this choice of N, ϵ is important for $B(\text{mG})<100$ while ϵ' contributes significantly for $B(\text{mG})>600$. We find that $\epsilon=4$ and $\epsilon'=12$ are required to fit the data; larger values cause too much upward curvature, and smaller ones do not cause enough.

2. Stokes–Einstein behavior

We summarize in Figs. 3–9 our results with the solvents: DNBPT, D_2O, decane, and dodecane, and the relevant parameters may be found in Table II, where they are compared with previous results with other solvents.

For DNBPT we could study the whole motional narrowing range from $\tau_R \approx 5$ ps (at 118.3 °C) down to $\tau_R \approx 1$

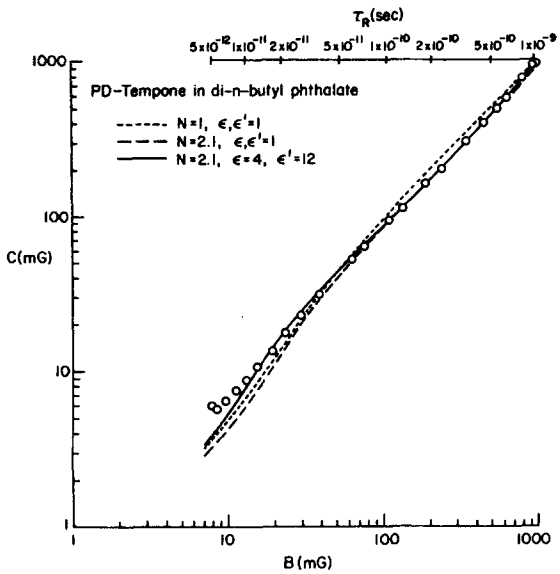

FIG. 3. Comparison of experimental and calculated values of C vs B for PD-Tempone in di-n-butyl phthalate.

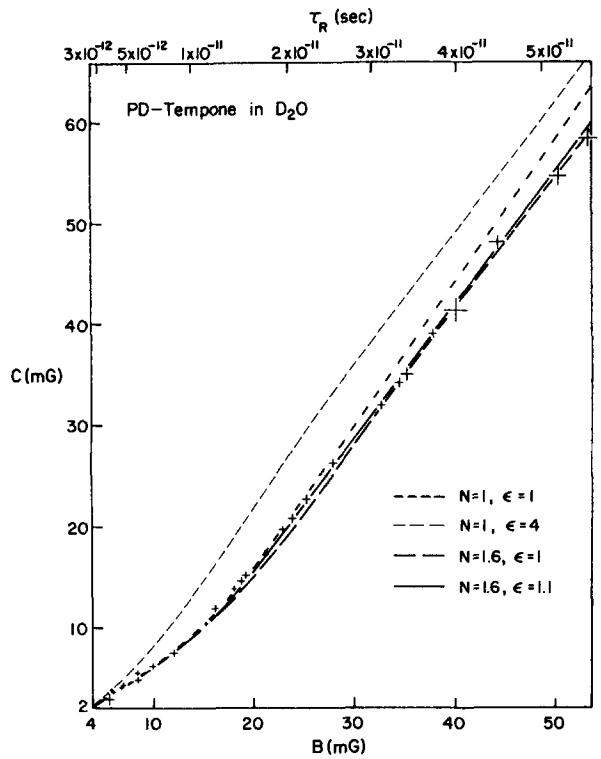

FIG. 5. Comparison of experimental and calculated values of C vs B for PD-Tempone in D_2O.

ns (at $-19\,^{\circ}C$). For D_2O the temperature range included the supercooled region to just below boiling (from $-12\,^{\circ}C$ to $96\,^{\circ}C$; the normal melting and boiling points of D_2O are 3.82° and $101.42\,^{\circ}C$).[24(b)] Motionally narrowed spectra were observed for PD-Tempone in the hydrocarbon solvents for temperatures ranging from well below the normal melting point to room temperature.

In general, Stokes–Einstein-type behavior [cf. Eq. (2)] is found for these solvents provided we use a modified form to allow for a nonzero intercept[5];

$$\tau_R = (4\pi\gamma_e^3\eta/3k_BT) + \tau_R^0 \ . \tag{6}$$

The slopes of τ_R vs η/T may be found in Table II expressed as an effective rotational radius γ_e. Alternatively, one can use a dimensionless "interaction parameter"[3(b)] $\kappa \equiv \gamma_e^3/\gamma_0^3$, where we take $\gamma_0 = 3.2$ Å as the geometric effective spherical radius of PD-Tempone.[1] (In Kivelson's notation there is also a molecular shape parameter λ which is unity for spheres. For asymmetric diffusion, it is related to our asymmetry parameter N.[1]) The intercepts τ_R^0 obtained from τ_R vs η/T plots are found to be negligible within experimental error for several cases, (cf. Table II), e.g., DNBPT, where it accurately describes the data over more than two orders of magnitude, as well as for D_2O where $\tau_R^0 = -0.2 \pm 2.8\times10^{-14}$ s is two orders of magnitude smaller than

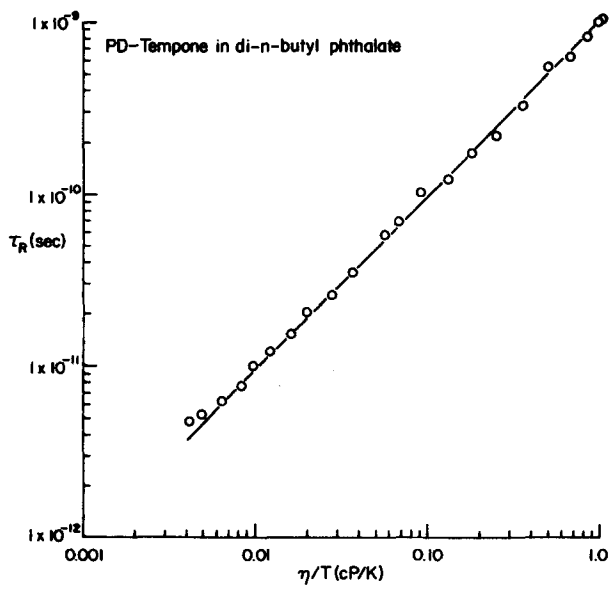

FIG. 4. τ_R vs η/T for PD-Tempone in di-n-butyl phthalate. The line is a least-squares-fit.

TABLE III. Temperature dependence of τ_R for PD-Tempone in several solvents.[a]

Solvent	a	Coefficient b in K	c in K^2
85% glycerol-$d3$-D_2O[b]	−10.3	-1.31×10^4	2.89×10^6
D_2O	−21.7	-4.51×10^3	1.04×10^6
di-n-butyl phthalate	−22.0	-5.19×10^3	1.40×10^6
toluene-$d8$[b]	−28.4	6.92×10^2	2.02×10^5
acetone-$d6$[b]	−29.5	8.40×10^2	4.95×10^4
ethanol-$d6$[b]	−30.1	1.18×10^3	8.13×10^4

[a]Coefficients of Eq. (7) obtained by least-squares-fits to the expression $\ln\tau_R = a + (b/T) + (c/T^2)$. Here $a = \ln\tau_R'$, $b = \Delta H_A^0/R$, $c = \Delta H_a'/R$.
[b]From Ref. 1.

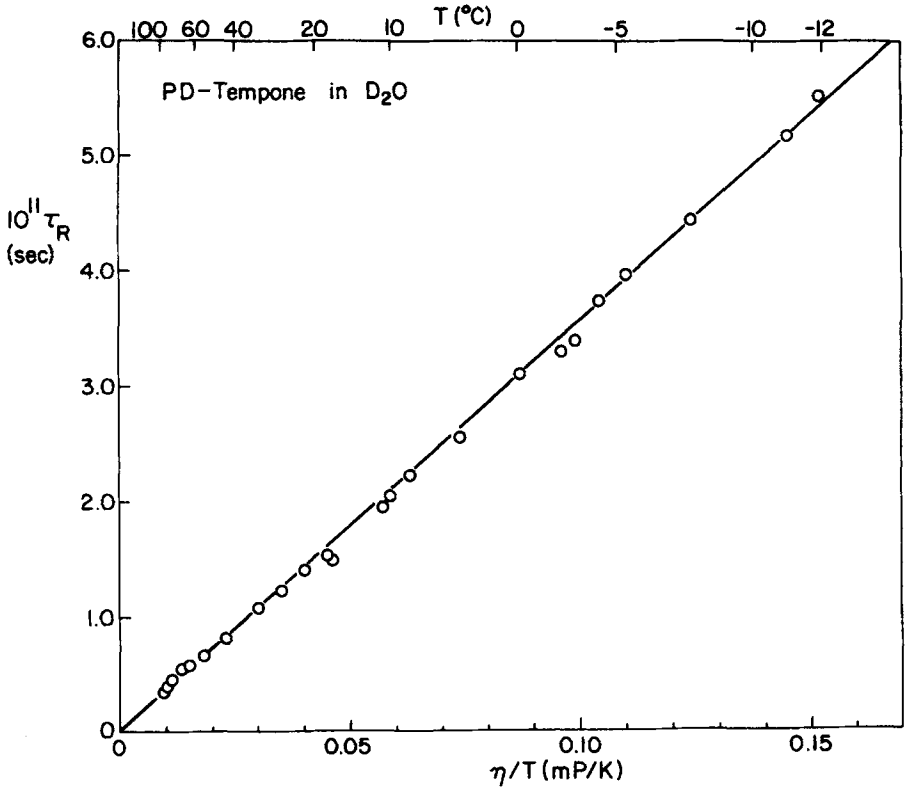

FIG. 6. τ_R vs η/T for PD-Tempone in D_2O. The line is a least-squares fit.

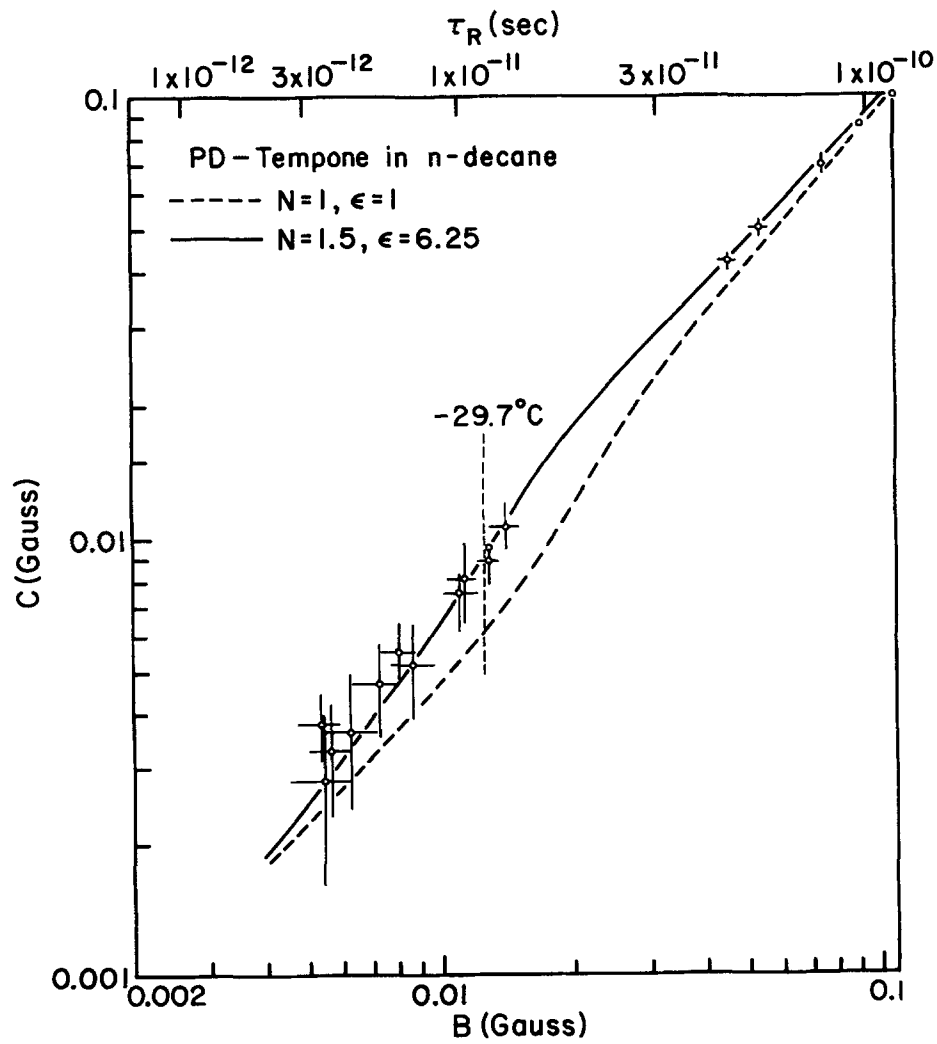

FIG. 7. Comparison of experimental and calculated values of C vs B for PD-Tempone in n-decane. (Normal mp $-29.7\,^{\circ}C$.)

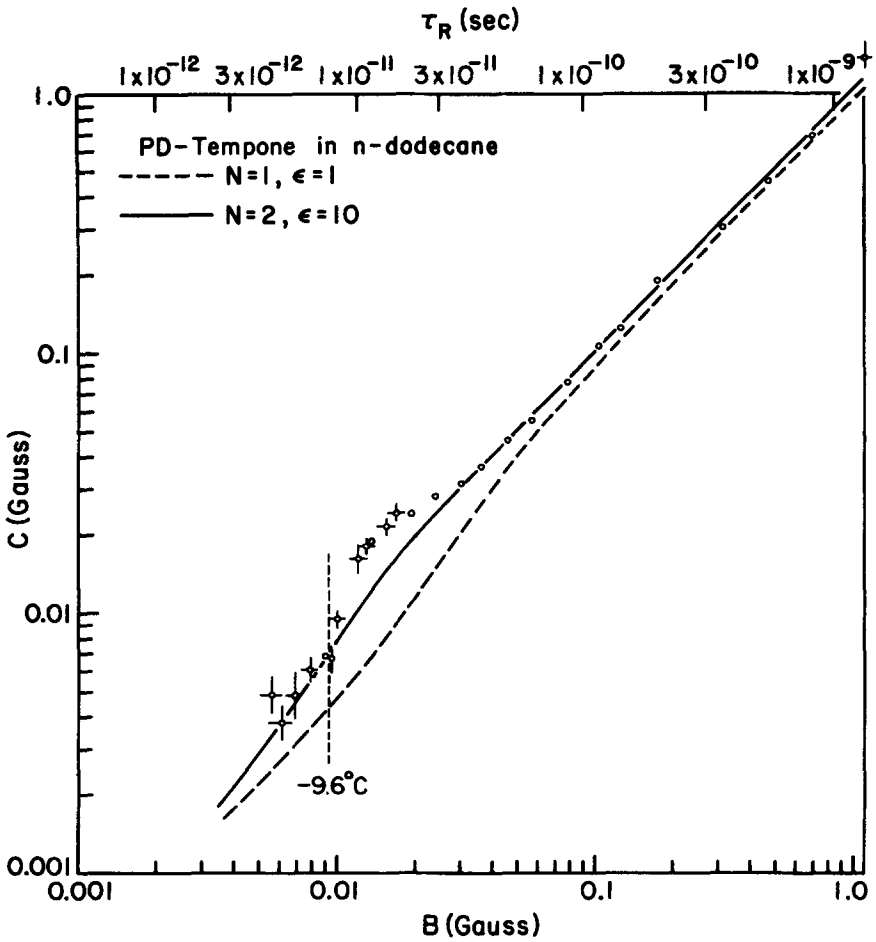

FIG. 8. Comparison of experimental and calculated values of C vs B for PD-Tempone in n-dodecane. (Normal mp -9.6 °C.)

the shortest measured τ_R. The values of τ_R^0 for decane and dodecane are, however, different from zero within experimental error, while the results of HMHF for acetone, ethanol, and glycerol/D_2O reanalyzed according to Eq. (6) show *negative* intercepts. Rigorous Stokes–Einstein behavior would require $\tau_R^0 = 0$. We shall defer to II,[9] a discussion of the implications of nonzero intercepts.

The modified Stokes–Einstein behavior with a $\kappa < 1$ appears to fit most of our results rather well. The values of κ show a correlation with molar volume of solvent, (cf. Table II) as would be expected from simple free-volume models.[5] That is, the space available for reorientation of the probe should depend upon the size of holes in the solvent and this can be expected to be a function of V_{probe}/V_s. One might also expect that there be a correlation with E_T, if we regard κ as a measure of the relative importance of intermolecular interactions.[3(b)] However, we do not observe a good correlation between κ and E_T in our results.

The dependence of N on solvent appears to demonstrate more specific features of the interaction between probe and solvent. Thus, hydrogen bonding solvents tend to show more rapid rotation about the molecular x axis, consistent with specific H bonding to the N–O and/or C=O functional groups of PD-Tempone, while for the long hydrocarbon (or liquid crystalline) solvents there is a tendency to more rapid y-axis rotation. The standard geometric arguments for PD-Tempone as a prolate nearly axially symmetric ellipsoid[25] (we have estimated[1] $a_x \cong 4.2$ Å, $a_y \cong 2.7$ Å, and $a_z \cong 3.0$ Å) lead to the prediction of $R_y/R_x \approx 3/4$.[1] (However, one should recall that the PD-Tempone spin-relaxation is most sensitive with respect to rotation about the x and y axes.) We do not find a correlation of N with either E_T or V_s. Some further comments on another mechanism which can have an apparent effect on N are made in Sec. IV.

3. Non-Debye spectral densities

We next consider the results for ϵ (cf. Table II and Figs. 3, 5, 7, and 8). The most interesting observation is that while $\epsilon > 1$ for DNBPT and for the hydrocarbons, consistent with our previous results on other solvents,[1] D_2O is the only case where we obtain an unequivocal result of $\epsilon \cong 1$. We also find a reasonable correlation between ϵ and E_T (cf. Fig. 10), which is interesting. (The correlation with V_s is not as good, but we suspect there is some correlation. There is a bias in the solvents we have used such that those with smaller E_T tend to have a large V_s, while those with larger E_T tend to have a small V_s.)

In general, a single ϵ is found to fit our data for each solvent rather well, but there are typical exceptions. Thus for DNBPT there is a tendency for the linewidth parameter C to level off to a constant value in the region $\tau_R < 5$ ps, a feature previously seen for PD-Tempone in

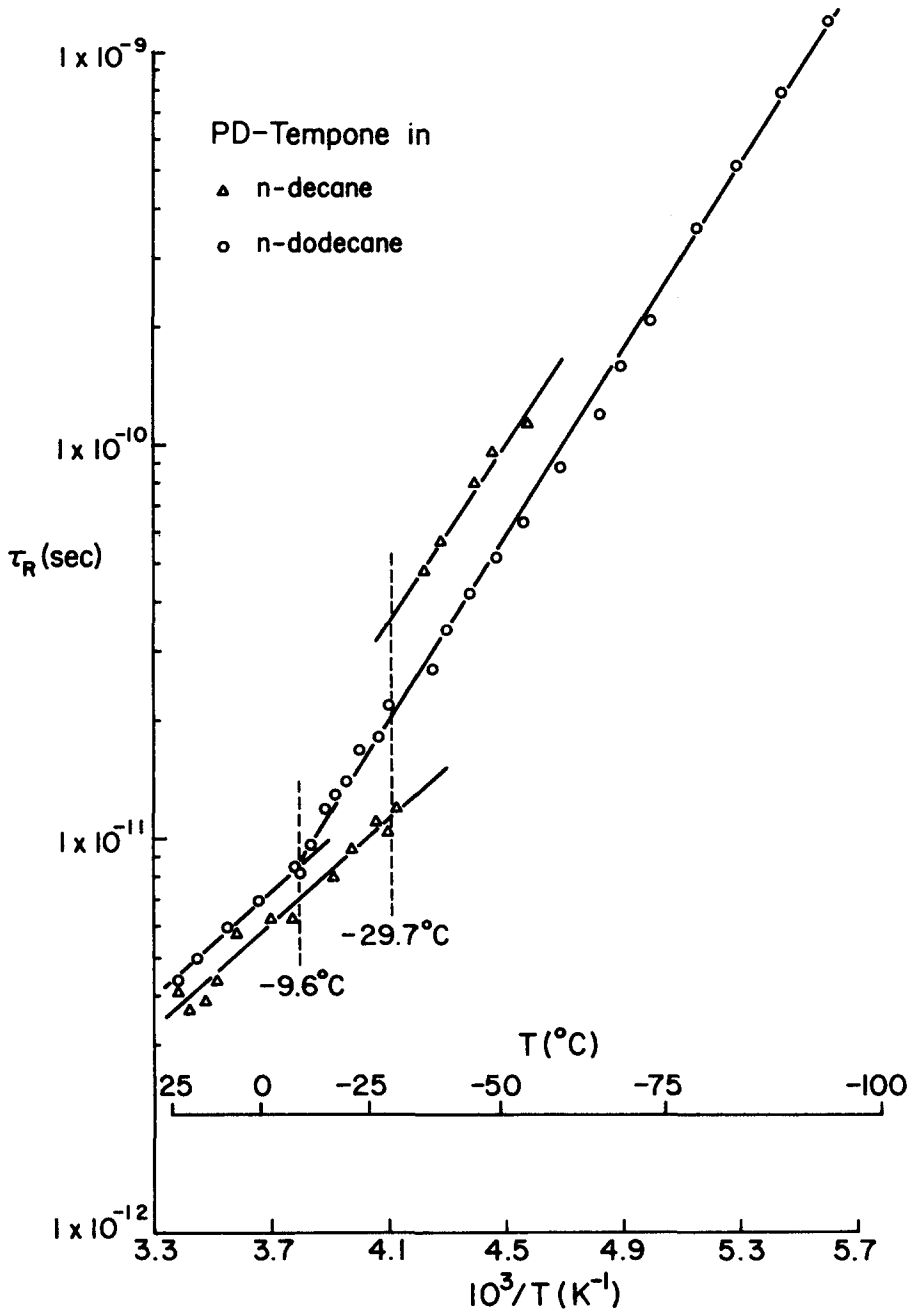

FIG. 9. τ_R vs $1/T$ for PD-Tempone in in n-decane and in n-dodecane.

toluene[1] for $\tau_R < 3$ ps, while B does not show a significant deviation. No such anomaly is observed for D_2O solvent in this region. It was suggested by HMHF that this width anomaly in C might be due to some intramolecular process which weakly modulates the hyperfine interaction. Our present results show this anomaly to be solvent dependent, perhaps due to a residual solvent modulation of the hyperfine interaction (either through direct interaction or else by affecting some intramolecular torsional motion).[25] The absence of an anomaly for D_2O might be explained by a more rapid relaxation-time for such a process.[26]

Another exception is observed for dodecane solvent where C/B is unusually large in the $\tau_R \sim 1 - 3 \times 10^{-11}$ s region. The discrepancy begins at approximately the normal melting point. The same results were obtained whether samples were cooled from above or warmed from below this temperature range. Effects somewhat similar to this were previously reported near the freezing point (as a function of pressure[7(c)]) for PD-Tempone in the viscous nematic solvent, Phase V (occurring at $\tau_R \sim 10^{-9}$ s), and it was suggested that this might be due to a mechanism related to the phase transition (cf. the SRLS mechanism discussed in Sec. IV A). A similar explanation might be appropriate here.

4. *Activation energies*

In general, the τ_R do not show a simple logarithmic dependence with $1/T$. Instead we found that the empirical form[27]:

$$\ln \tau_R = \ln \tau_R' + \Delta H_a / RT \ , \tag{7a}$$

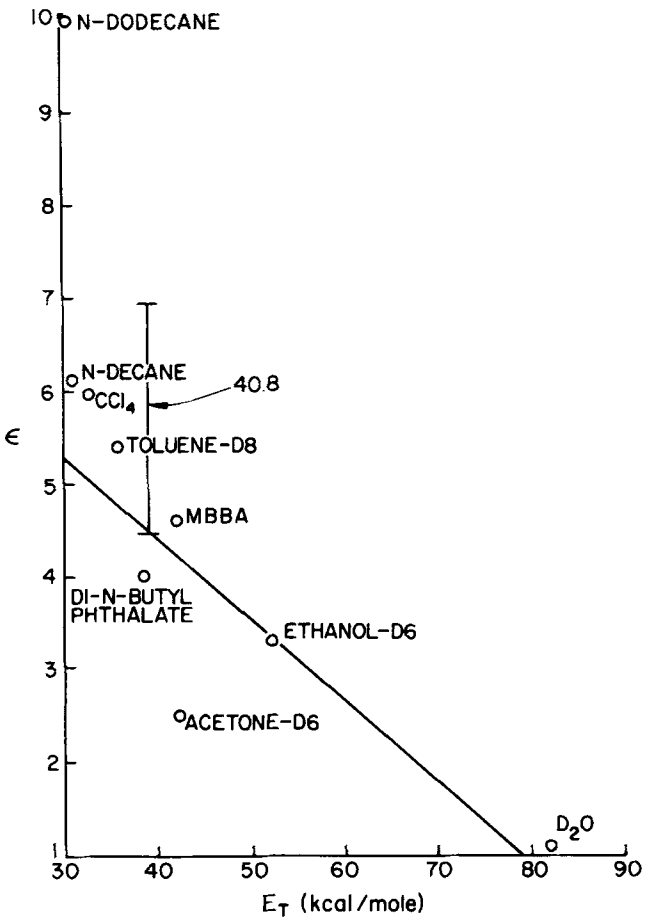

FIG. 10. ϵ vs E_T for PD-Tempone in several solvents. (The line is drawn to guide the eye.)

with

$$\Delta H_a = \Delta H_a^0 + \Delta H_a'/T \tag{7b}$$

leads to good fits to our results (cf. Table III). The variation of ΔH_a with τ_R is shown in Fig. 11 for most of the solvents. It emphasises two characteristic types of behavior. These curves show ΔH_a increasing with decreasing τ_R. One set exhibits a very weak variation in ΔH_a while the other shows a much stronger variation. In addition to their similarities in $\partial \Delta H_a/\partial \tau_R$, the members of each set are similar in their respective magnitudes of ΔH_a. (The first set exhibits very similar values of $\ln \tau_R^0$, while those of the second set are considerably smaller). In the case of decane and dodecane (not shown) ΔH_a is constant except for the discontinuity at the normal melting points.

Of course, the good correlation between τ_R and η/T, means that η/T for these solvents may also be represented by equations of the form of Eqs. (7) with behavior similar to that of Fig. 11. In fact, a variety of related expressions (including the Doolittle equation, see above), which are usually justified in terms of free-volume models, are frequently used to fit viscous behavior of liquids.[12] A perhaps more significant point we note is that Eqs. (3) and (4) lead to values of $\Delta H_a^{\eta/T}$ for η/T such that the ratio $\Delta H_a/\Delta H_a^{\eta/T}$ increases with decreasing T both for DNBPT and D_2O solvent (e.g., for DNBPT it is 0.91 at 120 °C, 0.98 at 50 °C, 1.01 at −20 °C, while for D_2O it is 0.81 at 95 °C and 1.02 at −10°). Such a gradual variation seems to cause little difficulty in obtaining good least-squares-fits of form of Eq. (2), but it does suggest some deviation from Stokes–Einstein behavior which are not apparent from Table II. These effects will be found to be more pronounced in the pressure-dependent study of II.[9]

5. *Spin-rotational relaxation*

The experimental linewidth coefficient A for PD-Tempone in di-*n*-butyl phthalate and in D_2O are shown as a function of τ_R in Figs. 12 and 13. The calculated values A_{dg} based upon dipolar and g-tensor terms leads to the dashed curves in Figures 12(a). The difference $A - A_{dg}$ is referred to as the residual linewidth A', and this quantity is treated as follows.

A simplified form of the spin-rotation derivative line-

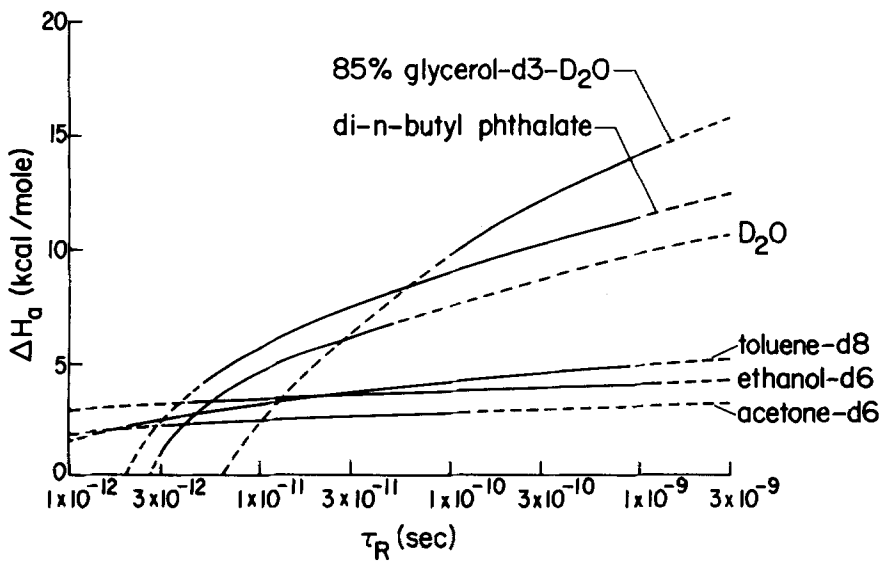

FIG. 11. ΔH_a vs τ_R for PD-Tempone in several solvents. The curves are described in Table III. Dashed segments are extrapolated results.

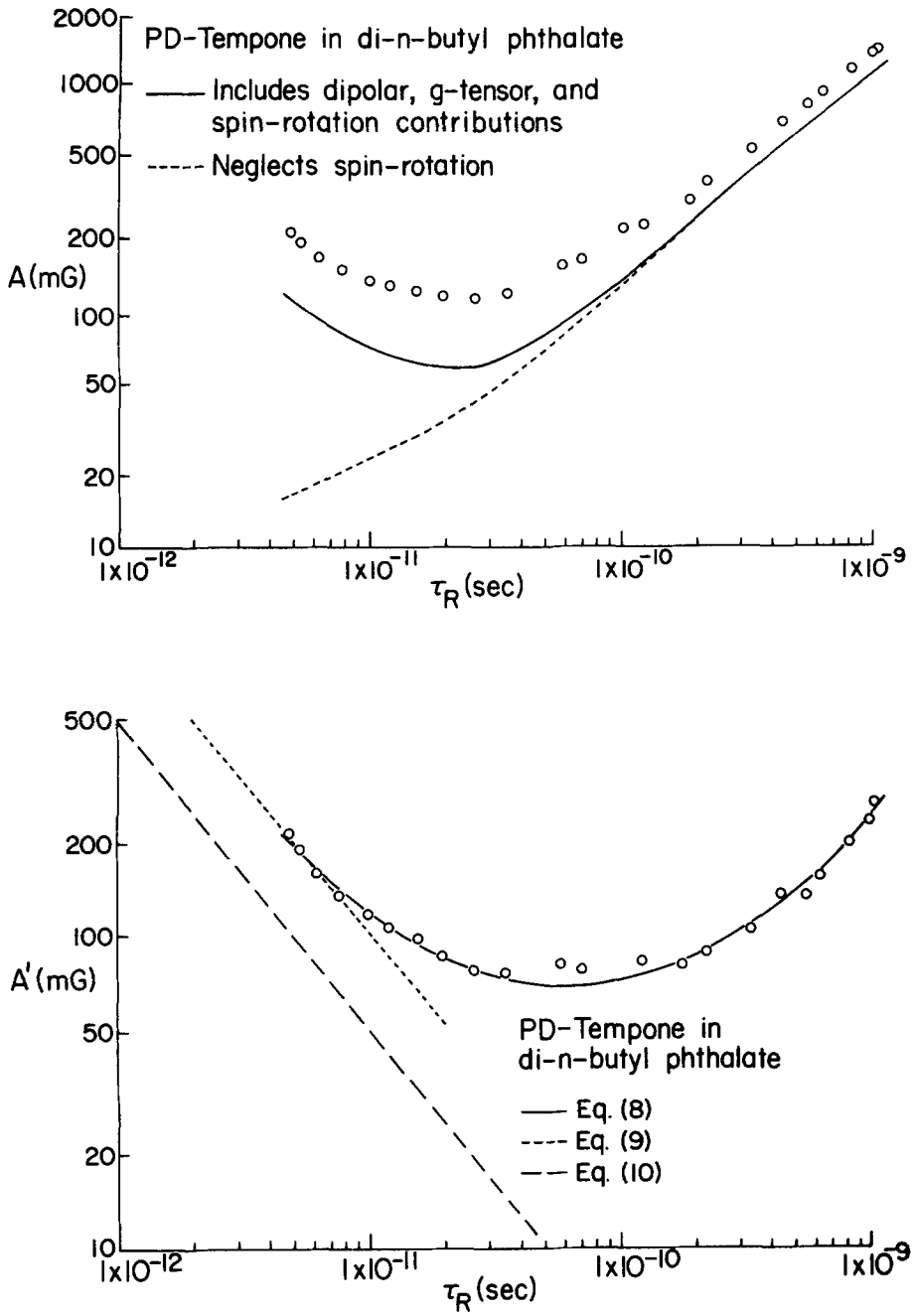

FIG. 12. (a) Comparison of experimental and calculated values of A vs τ_R for PD-Tempone in di-n-butyl phthalate. (b) Comparison of experimental and calculated values of A' vs τ_R for PD-Tempone in di-n-butyl phthalate.

width contribution for isotropic Brownian reorientation is [1,27]

$$A'_{SR} = \frac{2}{\sqrt{3}\gamma} \sum_i (g_i - g_e)^2 / 9\tau_R \ , \tag{8}$$

where γ is the electronic magnetogyric ratio and g_e is the electron free-spin g factor. The solid curve in Fig. 12(a) is the sum $A_{dd}+A'_{SR}$. The inclusion of the spin-rotation mechanism improves the qualitative agreement between experiment and theory, but quantitative differences are substantial, as is usually the case.[1] Figure 12(b) provides a closer look at these effects. Plotted against τ_R the residual linewidth A' exhibits a very broad minimum. The usual analysis calls for a fit of the high temperature data to the functional form

$$A' = A_1^2/\tau_R \ . \tag{9}$$

The short-dashed line in Fig. 12(b) is the least-squares result, $A_1^2 = (9.99 \pm 0.51) \times 10^{-13}$ G s for PD-Tempone in DNBPT. This is 2.05 times the corresponding coefficient calculated for spin-rotation relaxation through Eq. (8). (This value is virtually identical to that found for PD-Tempone in acetone-$d6$.[1])

The complete τ_R dependence of A' can be represented by

$$A' = \alpha/\tau_R + \beta\tau_R + \gamma \ , \tag{10}$$

where $\alpha = A_1^2$. In view of Eq. (8), the first term in Eq. (10) should represent a spin-rotation interaction. The second term accounts for any inaccuracies in A_{dd} that result from uncertainties in the parameters N, ϵ, ϵ', and τ_R as determined from the linewidth coefficients B and C for the rotational model used. It also includes

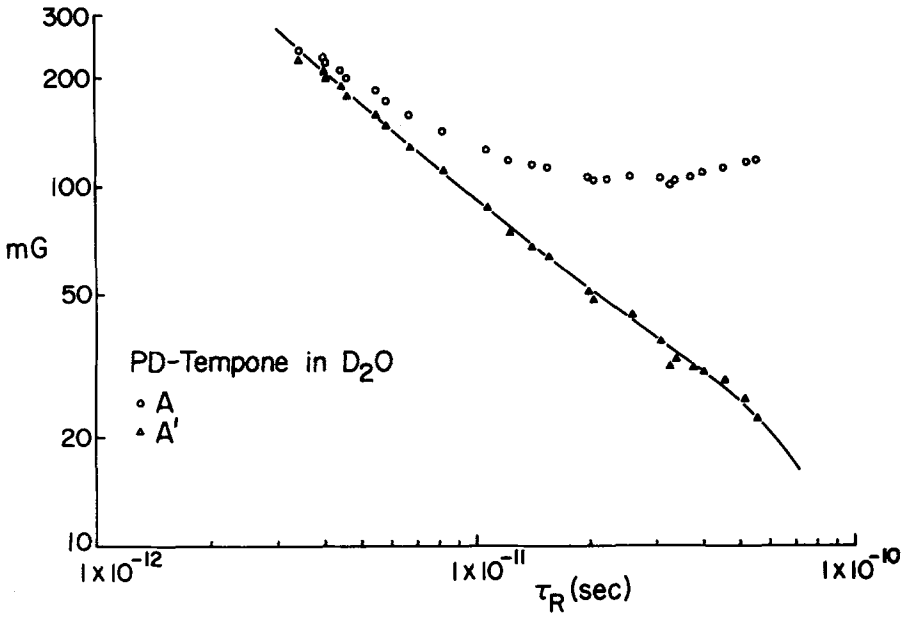

FIG. 13. A and A' vs τ_R for PD-Tempone in D_2O. The curve is a least-squares fit to Eq. (10).

electron–nuclear spin dipolar interactions.[1] The τ_R-independent term should include residual inhomogeneous broadening not accounted for by our analysis of intrinsic widths from the observed widths (possibly from magnetic field inhomogeneity and some residual unresolved hyperfine structure, see also Ref. 4). It could also include relaxation processes that are nearly temperature independent (e.g., possible intramolecular contributions to spin-rotational relaxation, cf. Ref. 1 and above).

We find for DNBPT solvent: [cf. Fig. 12(b)]:

$$A'(\text{mG}) = (7.30\pm 0.36)\times10^{-10}/\tau_R + (1.857\pm 0.071)\times10^{11}\tau_R + (46.9\pm 0.33) \quad (11)$$

and for D_2O solvent (cf. Fig. 13):

$$A'(\text{mG}) = (7.52\pm 0.15)\times10^{-10}/\tau_R - (1.82\pm 0.80)\times10^{11}\tau_R + (18.2\pm 3.0)\ . \quad (12)$$

Thus, by means of Eq. (10) both solvents yield very similar estimates for A_1^2, the effective spin-rotation factor of Eq. (9) and for DNBPT it is 1.5 times the prediction of Eq. (8) representing an improved agreement. The negative sign for the β term for D_2O solvent is surprising and inconsistent with previous results; it may simply be due to the fact that the data for PD-Tempone in D_2O are for $\tau_R \geq 5.5\times10^{-11}$ s, so there are insufficient results to obtain an accurate estimate of this term. However, in our analysis, the β-term, while somewhat uncertain, is still statistically significant. It could, of course, result from inaccuracies in A_{dz} as noted. Another possibility is one that follows from previous saturation measurements of the electron-spin-flip rate, W_e for PD-Tempone and PADS in other solvents.[1,2] In the high-temperature region it was found that $2W_e \approx A'$ consistent with a spin-rotational mechanism, but at lower temperatures $A' \gg 2W_e$, because of the β/τ_R term. This parameter W_e did show a downswing at lower temperatures (in these previous studies), and if A' for PD-Tempone in D_2O is showing this feature, it would be the first time that the usual positive contributions to β are very small.

For present purposes, the most important conclusion is that over the motional narrowing region studied here, the results on spin-rotational relaxation are consistent with the Hubbard–Einstein relation[28]:

$$\tau_R \tau_J = I/6kT = 1.45\times10^{-22}/T\ (\text{s}^2)\ , \quad (13)$$

upon which Eq. (8) is based. Then over the temperature range studied here, $\tau_J \ll \tau_R$, (e.g., for D_2O the smallest $\tau_R = 3.5$ ps at 96 °C, so from Eq. (13) $\tau_J = 0.11$ ps). Thus inertial effects are negligible over the range of rotational correlation times we have studied, and this justifies our neglect of them in our analysis of τ_R in terms of modified Stokes–Law models.

6. *Slow-motional spectra*

In HMHF it was shown that analysis of slow-motional line shapes of PD-Tempone can be used to distinguish the microscopic model for reorientation, i.e., whether the motion is Brownian, or jump, or an approximate "free diffusion" one. Only in the case of DNBP did we observe in the present work slow motional line shapes which were amenable to analysis. These were studied in the manner of HMHF, and it was found from simulations in the model-sensitive region ($\tau_R \sim 10^{-8}$ s) that while none of the models gave nearly as good agreement with experiment as HMHF obtained, the best agreement was found to be with the approximate free diffusion or with the moderate jump [with an $R\tau \sim 4$, cf. Ref. 2(a)], a result that is consistent with the results of HMHF on PD-Tempone in toluene-$d8$ and glycerol-d_3-D_2O solvent.

IV. FURTHER DISCUSSION

A. Non-Debye spectral densities

We wish to consider the observed correlation between ϵ and E_T. HMHF[1] presented an approximate theory for

ϵ, in which the fluctuating (or random) torques acting on the probe molecule were explicitly included in either a generalized or an augmented Fokker–Planck equation for the probe molecule. They could obtain a simplified expression for ϵ in the limit where $\tau_J/\tau_R \ll 1$ (i.e., neglect of the usual inertial terms) but where τ_M, the relaxation time of the torques is not necessarily much faster than τ_R. In particular, they obtained:

$$\epsilon \approx \left(1+\frac{\tau_M}{\tau_R}\right)^2 , \tag{14}$$

with

$$\tau_R = \tau_M\left(\frac{IV^2}{6k_BT}\right) , \tag{15}$$

and

$$\tau_J^{-1} = V^2\tau_M , \tag{16}$$

so that the Hubbard–Einstein relation Eq. (13) is obeyed. Here $(Ik_BT)\,V^2$ is the mean-square value of the fluctuating torques. Hwang and Freed[30(a)] presented a more detailed derivation of this result using a projection operator approach to generate the generalized rotational Fokker–Planck operator and then a functional derivative method to produce the lowest order contribution of the fluctuatin torques to a Smoluchowski equation. The method of the augmented Fokker–Planck equation outlined by HMHF yielded similar results, but illustrated some significant weaknesses of these results. Recently Stillman and Freed[30(b)] have considered the approach of augmented Fokker–Planck equations in detail, and have established a self-consistent method for creating and studying them. It is clear from these works that the above expressions for ϵ are really just lowest order results (in an expansion of $|V\tau_M|$) for a very simple model, even though they are then applied to results for which lowest order results are not really applicable. It is our belief that, while Eqs. (14)–(16) cannot be taken as quantitatively valid over the range to which we apply them, they provide a certain "qualitative insight" in examining experimental trends, and we use them in this spirit.[31]

Polnaszek and Freed,[7(a)] in studies on liquid-crystalline solvents found that they required $\tau_M/\tau_R > 1$ (for ϵ') for PD-Tempone, and this appears to be unphysical. Therefore, they introduced a modified point of view that they refer to as the slowly relaxing local structure (SRLS) model. In this model, the slowly fluctuating components of the anisotropic intermolecular potential are regarded as a local structure which persists for a mean time τ_x, and with respect to which the probe rotates, since $\tau_x \gg \tau_R$. Then, on this longer time scale τ_x, the local structure relaxes. This SRLS model was found to be particularly useful in dealing with PD-Tempone in liquid crystalline solvents.[7] It leads to a prediction that spectral densities become[7(a),7(c),30,32]

$$j_K(\omega) = j_K^D(\omega)\,(1-S_{l,K}^2) + \frac{S_{l,K}^2\,\tau_x}{1+\omega^2\tau_x^2} , \tag{17}$$

where $j_K^D(\omega)$ are the Debye-type spectral densities:

$$j_K^D(\omega) = \tau(K)/[1+\omega^2\tau(K)^2] . \tag{18}$$

Here $S_{l,K}$ is the Kth irreducible component of the local ordering tensor for the probe in the instantaneous potential of interaction with neighboring solvent molecules, and for our present purposes $K=0$ or ± 2 corresponding to a unique principal axis system for the molecular properties of PD-Tempone (cf. Fig. 1) for this fluctuating order parameter.[33] Also $\tau(K)^{-1} \equiv 6R_\perp + K^2(R_\parallel - R_\perp)$. Under conditions we can most simply write as $S_l^2 \ll \tau(K)/\tau_x \ll 1$, we have[7(a),7(b)] for each K

$$j_K(\omega) \approx j_K(0)/[1+\epsilon_k\,\omega^2\tau(K)^2] , \tag{19a}$$

[with $j_K(\omega=0) \approx \tau(K)$]

$$\epsilon_K \approx \left\{1+S_{l,K}^2[\tau_x/\tau(K)]^3\left(\frac{1+\omega^2\tau(K)^2}{1+\omega^2\tau_x^2}\right)\right\}\left[1+\left(\frac{\tau_x}{\tau(K)}\right)S_{l,K}^2\right]^{-2}$$

$$\xrightarrow{\omega^2\tau_x^2 \ll 1} \left[1+S_{l,K}^2\left(\frac{\tau_x}{\tau(K)}\right)^3\right]\Big/\left[1+\left(\frac{\tau_x}{\tau(K)}\right)S_{l,K}^2\right]^2$$

$$\xrightarrow{\omega^2\tau(K)^2 \gg 1} \left[1+S_{l,K}^2\left(\frac{\tau_x}{\tau(K)}\right)\right]^{-1} . \tag{19b}$$

We do wish to point out that spectral densities of the *form* of Eq. (17) with Eq. (18) may be written down quite generally for any relaxation process whose correlation function is expressed as the sum of two exponential decays (with e.g., decay constants $\tau(K)$ and τ_x). The SRLS model is one such model but one that we emphasize because we believe it to be physically relevant.[7,30,32]

We now inquire whether we can distinguish an ϵ of the form of Eqs. (14)–(16) (e.g., fluctuating torque model) from an ϵ of the form of Eqs. (19) (e.g., SRLS) on the basis of our experimental results. Equations (14)–(16) for the fluctuating torque model will lead to a nearly constant value of ϵ over the whole temperature range provided kT/IV^2 is only weakly temperature dependent compared to $\tau_{\bar R}$ [or $\tau(0)$ and $\tau(2)$]. Equations (17)–(19) for the SRLS model will lead to *different* results for ϵ in the two limits of extreme narrowing: $\tau_{\bar R}^2 \ll \tau_x^2 \ll \omega^{-2}$, and of slower tumbling (but still motional narrowing) $\tau_x^2 \gg \tau_{\bar R}^2 \gg \omega^{-2}$, with a more complex behavior between these two limits. It was suggested by Polnaszek and Freed[7(a)] that both $\tau_{\bar R}$ and τ_x are coupled to the same viscous modes represented by the shear viscosity η, so that $\tau_x/\tau_{\bar R}$ should only be weakly temperature dependent, and the same might be expected for S_l^2 (based on mean ordering of nematics and their temperature dependence).

We thus see that while both models lead to values of $\epsilon > 1$ required by our observations on ϵ in this work (and that of HMHF), there is a constancy in ϵ over the full range of $\omega\tau_R$ observed in most solvents that is best fit with Eq. (14). (More precisely, when $\omega^2\tau(K)^2 > 1$, the SRLS model predicts an $\epsilon < 1$, but $\epsilon > 1$ for faster motions.)

In the case of dodecane, an $\epsilon \sim 10$ would yield from Eq. (14) a $\tau_M > \tau_R$, which does not seem satisfactory. However, ϵ for a SRLS model should be decreasing with decreasing $\tau_{\bar R}$ except perhaps for an anomalous increase in τ_x/τ_R with decreasing temperature [cf. Eq. (19b)]. Also, it is likely that the SRLS mechanism affects $j_0(0)$ and $j_2(0)$ differently; (that is, in general $S_{l,\pm 2} \neq S_{l,0}$, and in particular for axial local ordering of the probe one has $S_{l,\pm 2} = 0$). This can lead to large *apparent* anisotropy

(i.e., $N \neq 1$) when the relaxation data are handled simply as in Sec. III[7] especially if $S_i^2[\tau_x/\tau(K)]$ is not small [as was assumed in Eqs. (19)]. We have not observed any $N \gg 1$ (or $\ll 1$) in this work (cf. Table II), but the weak N_y anisotropy observed for the hydrocarbons could be due to the effects of a SRLS mechanism, (e.g., for $\tau(0) = \tau(2)$ with axial local ordering, one has[7(c)] $N' \approx (3/2)[\tau'(0)/\tau(2) - 1/3]$ where $\tau'(0) \approx \tau(0) + S_{i,0}^2 \tau_x$ and N' is the *apparent* anisotropy).

We come now to the observed correlation of ϵ with E_T. For the fluctuating torque model, we have from Eqs. (14) and (15) that $\epsilon = (1 + 6kT/IV^2)^2$, so that an increase in V^2 (representing an increase in strength of intermolecular torques) will decrease ϵ. The correlation of ϵ with E_T shown in Fig. 10 is just the expected trend from the point of view of this model, viz., ϵ decreases with increased E_T, representing increased interaction between probe and solvent! For the SRLS model, we would expect to relate E_T to S_i^2, since S_i^2 is a measure of the local interaction potential between probe and solvent, and this would lead to ϵ increasing with E_T opposite to the observed correlation. One would have to consider the likelihood that τ_x is shorter for strongly interacting solvents, (and this effect dominates over solvent variation of S_i^2) in order to try to predict the correct trends. (Note, however, that larger solvent size should correlate well with increasing S_i^2 and τ_x.)

The fluctuating torque and SRLS models are based upon molecular descriptions of the rotational dynamics. One can examine whether more phenomenological hydrodynamic models might be of some use in the matter of non-Debye spectral densities. We previously pointed out[1] that the rotational Stokes model including the backflow effect[34] (which gives rise to the "long-time tails") could lead to an ϵ correction, but it is much too small, is of the wrong sign, and is very sensitive to η/T, so it is not consistent with our observations. However, the phenomenological introduction of viscoelastic effects into the viscosity,[35,38] e.g., by the Maxwell approximation: $\eta(\omega) = \eta_0/(1 - i\omega\tau_{VE})$, where τ_{VE} is a viscoelastic relaxation time, would lead to results formally equivalent to our fluctuating-torque model, but with[34] $\tau_M \to \tau_{VE}$ so

$$\epsilon \approx \left(1 + \frac{\tau_{VE}}{\tau_R}\right)^2$$

and $V^2 \tau_M \to 8\pi r_e^3 \eta_0/I$ for a Stokes–Einstein model. Our results would then be interpretable in terms of a *single* τ_{VE} consistent with the Maxwell approximation (except perhaps for dodecane) and for τ_{VE}/τ_R remaining constant as a function of temperature (for each solvent). This phenomenological description does not provide an explanation for the source of the viscoelasticity affecting the reorientation of the PD-Tempone probe, whereas the molecular theories outlined above do attempt this.

B. Effect of phase transitions in *n*-decane and *n*-dodecane

One of our observations reported in Sec. III is that rapid rotational motion persists in both *n*-decane and *n*-dodecane below their respective normal melting points. Nevertheless there are clear indications of a phase transition in the observed τ_R as shown in Fig. 9. Thus for PD-Tempone in *n*-decane there is a discontinuity in τ_R at about the melting point (−29.7 °C), but ΔH_a is constant and equal to 3.00 ± 0.16 kcal/mol above and 5.1 ± 0.4 kcal/mol below the melting point. For PD-Tempone in *n*-dodecane there is only a discontinuous change in slope of τ_R vs $1/T$ at the melting point (−9.6 °C) with constant values of ΔH_a of 3.01 ± 0.14 and 5.36 ± 0.09 kcal/mol above and below the melting point, respectively. From this we can conclude that the local environment sampled by the PD-Tempone molecule is very much the same in the two solvents in the same phase. The increase in activation energy upon freezing can be understood in terms of a change in the solvent cavity within which the spin probe rotates Since the density of the solid hydrocarbon is greater than that of the liquid, simple compression of the solvent cavity should restrict rotational motion and increase its activation energy.

This behavior is reminiscent of observations made for PD-Tempone in several liquid crystalline solvents,[7(c)] and we can take the point of view offered there to discuss the present results. The nematic-smectic *A* phase transition in the liquid crystals (40, 6) and (40, 8) was found to lead to a discontinuity in τ_R in the manner of *n*-decane in Fig. 9, while τ_R for PD-Tempone in the liquid crystal 8 CB showed a kink at this transition much like that seen for *n*-dedecane at its melting point. Arguing by analogy to the mechanism of expulsion of the spin probe observed in the $N - S_A$ transition, frozen *n*-decane and *n*-dodecane must involve different molecular packing efficiencies at the phase transition. The more dramatic effect at the phase transition is shown by the smaller solvent *n*-decane which is more likely to freeze into a regular crystalline form that differs greatly from the liquid. The larger *n*-dodecane molecule probably freezes more amorphously with a reduced packing effect on the PD-Tempone. These results are of some interest in comparing with results on liquid crystals [cf. Ref. 7(c)].

V. CONCLUSIONS

(1) Our temperature-dependent results on rotational correlation time, τ_R for PD-Tempone in a variety of solvents appear to be consistent with a simple Stokes–Einstein type of η/T dependence but with nonzero intercept for some solvents, and it can be either positive or negative. Also inertial effects should be negligible over the range of τ_R studied.

(2) The parameter ϵ introduced by Freed and coworkers to correct the Debye-type nonsecular spectral densities is generally found to represent the results very well for $\tau_R \gtrsim 5$ ps, i.e., a single ϵ is required for each solvent. A reasonable correlation between ϵ and the solvent molar transition energy E_T (which is a good measure of specific solvent polarity) was found. That is, as solute-solvent interactions become weaker, ϵ increases from its Debye limit of unity. Only in the case of D_2O solvent has this limit been observed so far

for PD-Tempone. These results appear consistent with the fluctuating-torque model previously used by Freed and co-workers, although the model must be regarded as a very approximate one.

(3) A useful method of interpolation to obtain the solvent dependence of the PD-Tempone magnetic tensors is described. It is based on the good correlation of these tensor components with the molar transition energy E_T. This method should be useful for other spin probes (e.g., nitroxides, vanadyl complexes, etc.), and it reduces the need for extensive rigid limit simulations.

[1]J. S. Hwang, R. P. Mason, L. P. Hwang, and J. H. Freed, referred to as HMHF, J. Phys. Chem. **79**, 489 (1975).

[2](a) S. A. Goldman, G. V. Bruno, C. F. Polnaszek, and J. H. Freed, J. Chem. Phys. **56**, 716 (1973); (b) S. A. Goldman, G. V. Bruno, and J. H. Freed, J. Chem. Phys. **59**, 3071 (1973).

[3](a) R. Wilson and D. Kivelson, J. Chem. Phys. **44**, 154 (1966); (b) B. Kowert and D. Kivelson, J. Chem. Phys. **64**, 5206 (1976).

[4]R. F. Campbell and J. H. Freed, J. Phys. Chem. **84**, 2668 (1980).

[5](a) D. Kivelson and P. Madden, Annu. Rev. Phys. Chem. **31**, 523 (1980); (b) J. L. Dote, D. Kivelson, and R. N. Schwartz, J. Phys. Chem. **85**, 2169 (1981).

[6]W. A. Steele, Adv. Chem. Phys. **34**, 1 (1976).

[7](a) C. F. Polnaszek and J. H. Freed, J. Phys. Chem. **79**, 2283 (1975); (b) J. S. Hwang, K. V. S. Rao, and J. H. Freed J. Phys. Chem. **80**, 1790 (1976). A summary of the various reorientational models may be found in this work; (c) W. J. Lin and J. H. Freed, J. Phys. Chem. **83**, 379 (1979).

[8]C. Reichardt, Angew. Chem. Internat. Edit. **4**, 29 (1965). The E_T scale is based upon the use of pyridinium N-phenolbetaine, which exhibits a very large displacement of its solvatochromic band in different solvents. Thus E_T (kcal/mol) $=2.86\times10^{-3}\tilde{\nu}$, where $\tilde{\nu}$ is the absorption maximum in cm^{-1}.

[9]S. A. Zager and J. H. Freed, J. Chem. Phys. **77**, 3360 (1982).

[10]S. A. Zager, Ph.D. thesis, Cornell University, 1981.

[11]H. D. Connor, Ph.D. thesis, Cornell University, 1972.

[12]A. J. Barlow, J. Lamb, and A. J. Matheson, Proc. R. Soc. London Ser. A **292**, 322 (1966).

[13]G. S. Kell in *Water A Comprehensive Treatise*, edited by F. Franks (Plenum, New York, 1972).

[14]F. J. Millero, R. Dexter, and E. Hoff, J. Chem. Eng. Data **16**, 85 (1971).

[15]R. C. Hardy and R. L. Cottington, J. Res. Natl. Bur. Stand. **42**, 573 (1949).

[16]T. Defries and J. Jonas, J. Chem. Phys. **66**, 5393 (1977).

[17]American Petroleum Inst. Res. Project 44, Nat. Bur. Stand. Circ. **461**, 109 (1947); E. B. Giller and H. G. Drickamer, Ind. Eng. Chem. **41**, 2067 (1949); M. K. Karapetyants and Y. Kuo-sen, Russ. J. Phys. Chem. **37**, 1106 (1963).

[18]P. R. Bevington, *Data Reduction and Error Analysis for the Physical Sciences* (McGraw-Hill, New York, 1969).

[19](a) R. Lefebvre and J. Maruani, J. Chem. Phys. **42**, 1480 (1965); (b) C. F. Polnaszek, Ph.D. thesis, Cornell University, 1976.

[20]V. P. Golikov and V. I. Muromtsev, Zh. Strukt, Khim. **13**, 332 (1972).

[21]C. F. Polnaszek, S. Schreier, K. W. Butler, and I. C. P. Smith, J. Am. Chem. Soc. **100**, 8223 (1978).

[22]C. Jolicoeur and H. L. Friedman, Ber. Bunsenges. Phys. Chem. **75**, 248 (1971); J. Sol. Chem. **3**, 15 (1974); **7**, 813 (1978).

[23]F. Barbarin, J. P. Germain, and C. Fabre, Mol. Cryst. Liq. Cryst. **39**, 199 (1977).

[24](a) In special cases where this analysis fails then τ_R is simply given as the value calculated from the B linewidth coefficient, since it is found to be less sensitive to the details to the model used (Refs. 1, 2, and 7); (b) *CRC Handbook of Chemistry and Physics*, edited by R. C. Weast (CRC, Cleveland, 1973).

[25]X-ray studies summarized by J. Lajzerowicz-Bonneteau in *Spin Labeling Theory and Applications*, edited by L. J. Berliner (Academic, New York, 1976), Chap. 6, shows that Tempone is planar in the solid state. (More precisely, the N–O and C=O fragments lie in the *mean plane*, i.e., the N–O bond makes 0° angle with the CNC plane, although the six-member ring is in a twisted boat conformation). Bullock and Howard [J. Chem. Soc. Faraday Trans 1, **76**, 1296 (1980)] have concluded from an analysis of da_N/dT that Tempone (and other nitroxides) which are planar in the solid state seem also to be planar in solution, although they cannot rule out a pyramidal distortion with a very low barrier to inversion from studying da_N/dT alone.

[26]One observation that might contradict the ϵ analysis was a linewidth study for O^{17} labeled PADS (peroxylamine disulfonate) anion in H_2O [Ref. 2(b)]. In that work the analysis of O^{17} hfs linewidths suggested that $\epsilon\sim1$ while that for the N^{14} hfs linewidths suggested that $\epsilon\sim4$. However, the O^{17} hf tensor is large enough that one must use higher-order perturbation corrections in the manner of Wilson and Kivelson [Ref. 3(a)], but this was not done in the previous study. We have reanalyzed the B_0 and C_0 terms using such higher-order corrections, and we find that they yield $4.5<N<6$ and $4<\epsilon<6$ which is in reasonably good agreement with the N^{14} values of $N=4.7\pm1$, $\epsilon=4$. We also believe that the A_0 linewidth parameter was not obtained very accurately by Goldman *et al.* [Ref. 2(b)] because of extra spin-exchange broadening of the rather concentrated O^{17} labeled sample versus the more dilute unlabeled sample. The details of this reanalysis may be found in Ref. 10.

[27]A. J. Barlow, J. Lamb, and A. J. Matheson, Proc. R. Soc. London Ser. A **292**, 322 (1966).

[28](a) P. W. Atkins and D. Kivelson, J. Chem. Phys. **44**, 169 (1966); R. E. D. McClung and D. Kivelson, J. Chem. Phys. **49**, 3380 (1968). (b) P. S. Hubbard, Phys. Rev. **131**, 1155 (1963).

[29]We wish to thank Mr. Yishay Manassen for his extensive help with these simulations.

[30](a) L. P. Hwang and J. H. Freed, J. Chem. Phys. **63**, 118 (1975); (b) A. E. Stillman and J. H. Freed, J. Chem. Phys. **72**, 550 (1980) and (to be published).

[31]Similar criticisms apply to the simpler Kivelson–Keyes approach [J. Chem. Phys. **57**, 4599 (1972)].

[32]J. H. Freed, J. Chem. Phys. **66**, 4183 (1977).

[33]In our earlier work (Refs. 7 and 32) we have usually assumed cylindrically-symmetric local ordering of the probe, so $S_{I,k}=S_I\delta_{K,0}$. However, Lin and Freed [cf. Ref. 7(c), Appendix (B)] have generalized this result. Equations (21) and (22) are actually for $S^2_{I,K}\ll1$ (Ref. 32) and we have neglected cross terms of type: $S_{I,K}S_{I,K'}$ for $K\neq K'$ [Ref. 7(c)].

[34]L. D. Landau and E. M. Lifshitz, *Fluid Mechanics* (Pergamon, London, 1959), p. 97.

[35]J. Frenkel, *Kinetic Theory of Liquids* (Oxford University, London, 1946).

[36](a) R. Zwanzig and M. Bixon, Phys. Rev. A **2**, 2005 (1970); (b) T. S. Chow, J. Chem. Phys. **61**, 2868 (1974).

[37]Actually these forms for τ_R and ϵ are based upon having $\tau_R\gg\tau_J$, so inertial effects are negligible in the rotational reorientation. We have already shown this to be true for the experiments reported here. More precisely the approximation used is that the frequency-dependent rotational diffusion

coefficient

$$D_R(\omega) = (kT/I)\,[\beta(\omega) - i\omega]^{-1}$$

$$= \frac{kT}{I\beta(\omega)} \sum_{n=0}^{\infty} \left(\frac{i\omega}{\beta(\omega)}\right)^n, \quad \text{for } |\omega| < \beta(\omega),$$

$$\approx kT/I\beta(\omega), \quad \text{for } |\omega| \ll \beta(\omega),$$

[where $\beta(\omega)$ is the frequency-dependent friction coefficient and $\beta(0) \equiv \tau_J^{-1}$]. This is the approximation made by HMHF[1] and by Hwang and Freed (Ref. 29).